Macroporous and nanofibrous polymer scaffolds and polymer/bone-like apatite composite scaffolds generated by sugar spheres

Guobao Wei,[1] Peter X. Ma[1,2,3]
[1]*Department of Biomedical Engineering, University of Michigan, Ann Arbor, Michigan, 48109-2209*
[2]*Department of Biologic and Materials Sciences, University of Michigan, Ann Arbor, Michigan, 48109-1078*
[3]*Macromolecular Science and Engineering Center, University of Michigan, Ann Arbor, Michigan, 48109-1055*

Received 26 October 2005; revised 7 December 2005; accepted 22 December 2005
Published online 24 April 2006 in Wiley InterScience (www.interscience.wiley.com). DOI: 10.1002/jbm.a.30704

Abstract: Scaffolds are crucial to tissue engineering/regeneration. In this work, a technique combining a unique phase-separation process with a novel sugar sphere template leaching process has been developed to produce three-dimensional scaffolds. The resulting scaffolds possess high porosities, well connected macropores, and nanofibrous pore walls. The technique advantageously controls macropore shape and size by sugar spheres, interpore opening size by assembly conditions (time and temperature of heat treatment), and pore wall morphology by phase-separation parameters. The bioactivity of a macroporous and nanofibrous poly(L-lactic acid) (PLLA) scaffold was demonstrated by the bone-like apatite deposition throughout the scaffold in a simulated body fluid (SBF). Preincorporation of nanosized hydroxyapatite eliminated the induction period and facilitated the apatite growth in the SBF. Interestingly, the apatite growth primarily occurred on the surface of the pores (internal and external) but not the interior of the nanofibrous network away from the pore surface. It was also noticed that the macropore size did not affect the apatite growth rate, while the interpore opening size did. The compressive modulus also increased substantially when a continuous apatite layer was formed on the pore walls of the scaffold. The resulting composite scaffold mimics natural bone matrix with the combination of an organic phase (a polymer such as PLLA) and an inorganic apatite phase. The demonstrated bioactivity of apatite layer, together with well-controlled macroporous and nanofibrous structures, makes the novel nanocomposite scaffolds desirable for bone tissue engineering. © 2006 Wiley Periodicals, Inc. J Biomed Mater Res 78A: 306–315, 2006

Key words: scaffold; nano fiber; apatite; matrix; polymer; composite; sugar

INTRODUCTION

Strategies for bone tissue engineering are generally based on either the implantation of a porous scaffold to harness the natural progression of osseous growth or the seeding of osteogenic cells onto a three-dimensional (3D) scaffold followed by *in vivo* implantation to repair bone defects. In both cases, the scaffold serves as a temporary physical support and template for initial cell attachment, and it provides a microenvironment appropriate for further osteogenesis.[1,2] The development of appropriate 3D scaffolds for the maintenance of cellular viability and phenotype is critical and has been a challenge in the field of tissue engineering.[3–6] Scaffold materials must meet certain physical and biological criteria for tissue engineering applications. In terms of physical properties, an ideal scaffold should have three-dimensionally well-connected macropore structure to accommodate cells and to facilitate cell migration, proliferation, and differentiation, thereby ensuring functional neotissue formation. Consequently, scaffolds with high porosity and interconnected pore structures generally favor tissue regeneration.[7,8]

The surface morphology has been demonstrated to play a significant role in regulating cell activities such as attachment, proliferation, and/or differentiation.[9,10] Polymeric scaffolds with a nanofibrous pore wall architecture improved initial osteoblastic cell attachment (24 h) as compared to those with relatively smooth pore walls, possibly due to the selective adsorption of fibronectin and vitronectin on a nanofibrous scaffold.[9]

In previous studies, we used paraffin spheres to fabricate porous scaffolds. The main advantage of using paraffin spheres as a porogen (pore-generating material) is that, unlike other porogens (such as so-

Correspondence to: P. X. Ma; e-mail: mapx@umich.edu

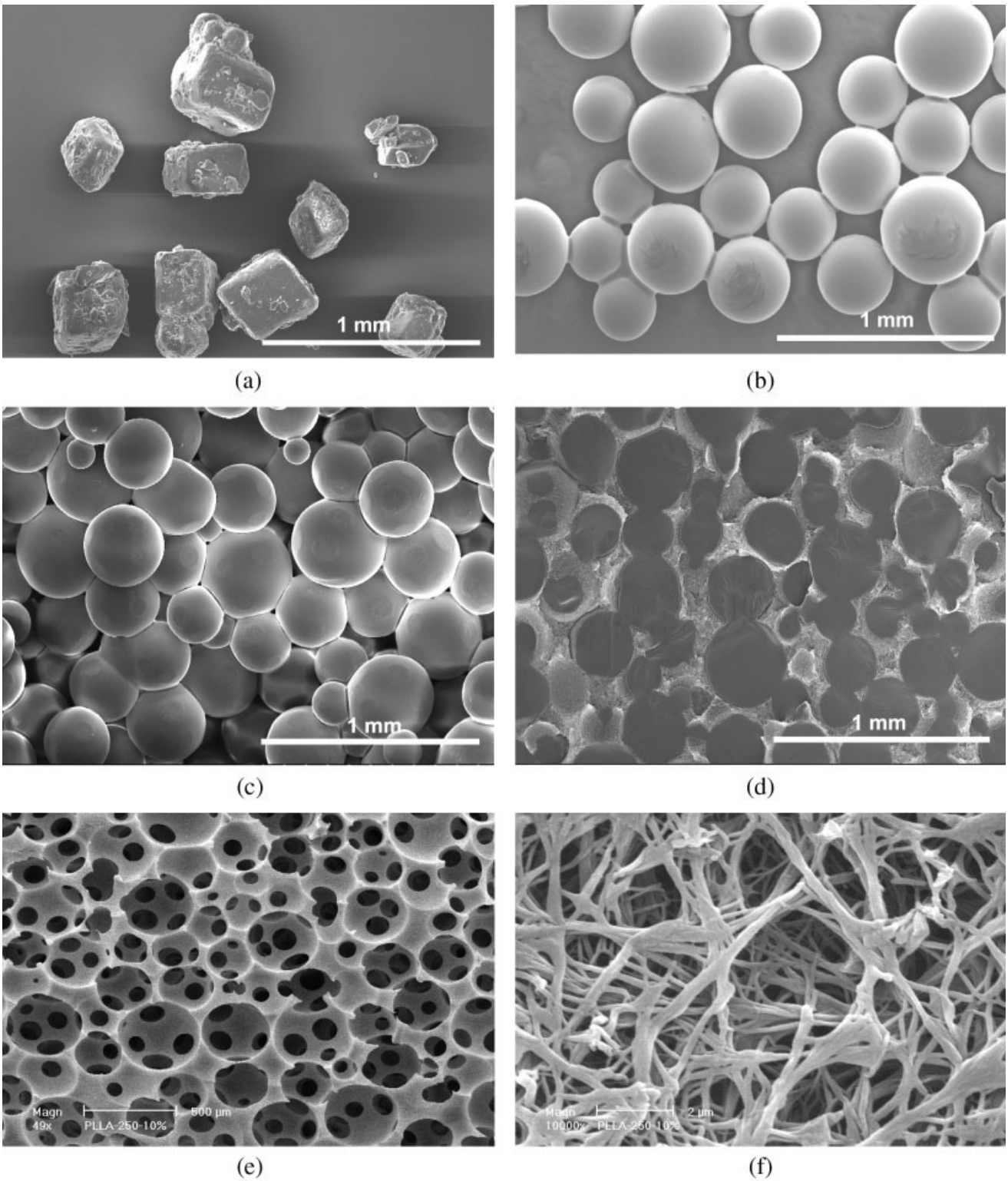

Figure 1. Fabrication process of sugar sphere template leaching and thermally induced phase separation technique, shown by SEM micrographs: (a) sugar particles as received (250–425 μm); (b) sugar spheres (250–425 μm) prepared via emulsion technique; (c) sugar sphere template after heat treatment at 37°C for 15 min; (d) polymer/sugar composite after polymer casting, phase separation, solvent exchange, and freeze-drying; (e, f) 3D macroporous and nanofibrous scaffold at low (×50) and high (×10,000) magnifications.

dium chloride crystals), they can be heat treated to form a bound template, thus creating interconnected pore openings in the final scaffolds. However, there are also some disadvantages of using paraffin spheres because many organic solvents such as tetrahydrofuran (THF), dioxane, dichloromethane, and pyridine

TABLE I
Structures of Macroporous and Nano-Fibrous Scaffolds

Scaffolds	Macropore size (μm)	Assembly condition (T, t)	Porosity (%)	Interpore opening size (μm)	Interpore opening area ratio (%)
PLLA180[a]	180–250	37°C, 15 min.	97.8	71.2 ± 13.1	22.4
PLLA250[b]	250–425	NT*	97.0	56.9 ± 14.9	4.8
PLLA250	250–425	37°C, 15 min.	97.8	116.5 ± 20.0	18.9
PLLA250	250–425	37°C, 30 min.	98.0	125.7 ± 31.5	24.6
PLLA250	250–425	57°C, 15 min.	98.2	129.1 ± 39.8	28.7
PLLA425[c]	425–600	NT*	96.9	75.0 ± 14.1	3.9
PLLA425	425–600	37°C, 15 min.	97.7	157.8 ± 39.3	22
PLLA425	425–600	37°C, 30 min.	97.8	165.4 ± 28.7	24.9
PLLA/nHAP250[d]	250–425	37°C, 15 min.	97.5	106.3 ± 16.7	17.6

[a]PLLA scaffold prepared using sugar spheres, 180–250 μm in diameter.
[b]PLLA scaffold prepared using sugar spheres, 250–425 μm in diameter.
[c]PLLA scaffold prepared using sugar spheres, 425–600 μm in diameter.
[d]PLLA/nHAP composite scaffold prepared using sugar spheres, 250–425 μm in diameter.
*NT—No heat treatment.

used for polymer dissolution also have varying degrees of solubility to paraffin. Therefore, paraffin spheres are not an ideal porogen for these systems. In addition, trace amount of paraffin could be left in the scaffolds, which could be unfavorable for the subsequent cell activity due to its hydrophobicity. In this work, we developed alternative sugar spheres to prepare 3D macroporous and nanofibrous scaffolds. Such scaffolds retained the advantages of interconnected spherical pores while avoiding the use of paraffin. Sugar is water soluble, allows removal without using organic solvents, and is suitable for the fabrication of scaffolds from any water insoluble polymers.

Because hydroxyapatite (HAP) is the major mineral phase in natural bone, coating a thin layer of HAP onto a metallic or polymeric material surface has been utilized to induce faster biological fixation of implants to host bone tissue.[11,12] For bone tissue engineering, the scaffold should also provide desired osteoconductivity[13,14] and mechanical properties.[15–17] The bioactivity of the new scaffold was demonstrated using *in vitro* bone-like apatite particle growth in a simulated body fluid (SBF). The apatite growth on the nanofibrous scaffolds also improved the mechanical properties. Therefore, the resulting novel polymer/apatite composite scaffolds should be advantageous for bone tissue engineering.

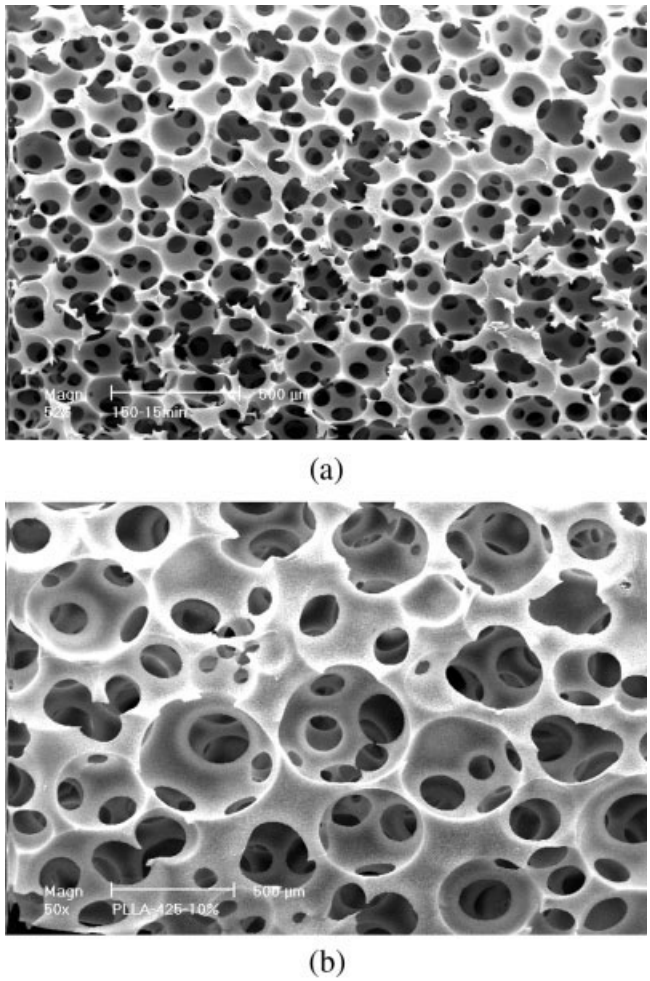

Figure 2. SEM micrographs of 3D nanofibrous PLLA scaffolds with varying macropore sizes: (a) 180–250 μm; (b) 425–600 μm. The magnification is ×50.

MATERIALS AND METHODS

Poly(L-lactic acid) (PLLA) with an inherent viscosity of 1.4–1.8 dl/g was purchased from Boehringer Ingelheim (Ingelheim, Germany) and was used as received. Hydroxyapatite nanocrystals (nHAP) were purchased from Berkeley Advanced Biomaterials (San Leandro, CA). D-fructose (m.p. 119–122°C), mineral oil, and sorbitanmonooleate (Span 80)

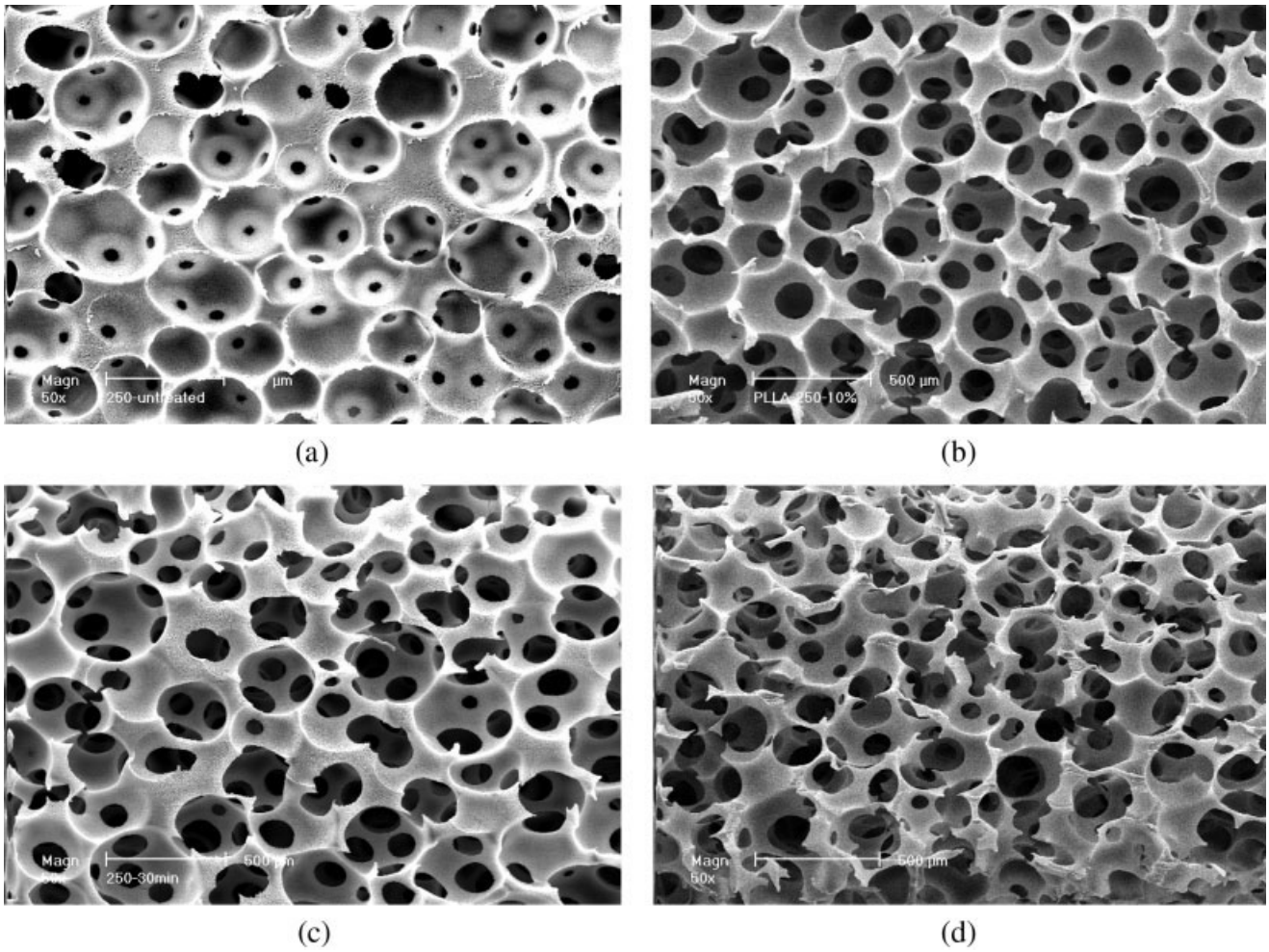

Figure 3. SEM micrographs of 3D nanofibrous PLLA scaffolds with varying interpore opening ratios (IOR) under different assembling conditions: (a) without heat treatment (4.8%); (b) 37°C for 15 min (18.9%); (c) 37°C for 30 min (24%); (d) 57°C for 15 min (29.1%).

were from Sigma (St. Louis, MO). Cyclohexane and hexane were from Fisher Scientific (Pittsburgh, PA). THF and all other chemicals were from Aldrich Chemical Company (Milwaukee, WI).

Preparation of sugar spheres

Sugar spheres with different sizes were prepared by an emulsion technique. Typically, 50 g of D-fructose were melted at 120°C for 90 min until clear yellowish liquid was obtained. The liquefied sugar was emulsified into 50 mL mineral oil with 1.3 mL Span 80 at 120°C under stirring. The resulting mixture was cooled down using an ice-bath to solidify sugar spheres. After discarding the mineral oil, the sugar spheres were washed with hexane three times and sieved to select desired sizes (180–250, 250–425, and 425–600 μm size ranges). The sieved sugar spheres were packed in a Teflon vial with hexane and heat treated for a certain time period to form a sugar sphere template. After bonding the sugar spheres, hexane was removed, and the sugar template was dried under vacuum.

Polymer casting and phase separation

The phase separation procedure for fabrication of porous scaffold was modified from Ma and Zhang.[4,18] Briefly, about 0.6–0.8 mL 10% PLLA/THF solution or PLLA/nHAP/THF suspension was cast into the assembled sugar template. Mild vacuum was applied during casting in order to fully fill the interspaces of the bonded sugar template with polymer solution. The polymer solution/sugar template was phase separated at −20°C overnight and then immersed into cyclohexane to extract solvent (THF) for 2 days. The resulting composites were freeze-dried. The sugar template was then leached away in distilled water, and the highly porous nanofibrous scaffold was freeze-dried.

Bone-like apatite deposition

Prefabricated nanofibrous scaffolds were incubated in a 1.5× SBF with a modified formulation that was prepared by dissolving NaCl, $NaHCO_3$, KCl, $K_2HPO_4{\cdot}3H_2O$, $MgCl_2{\cdot}6H_2O$,

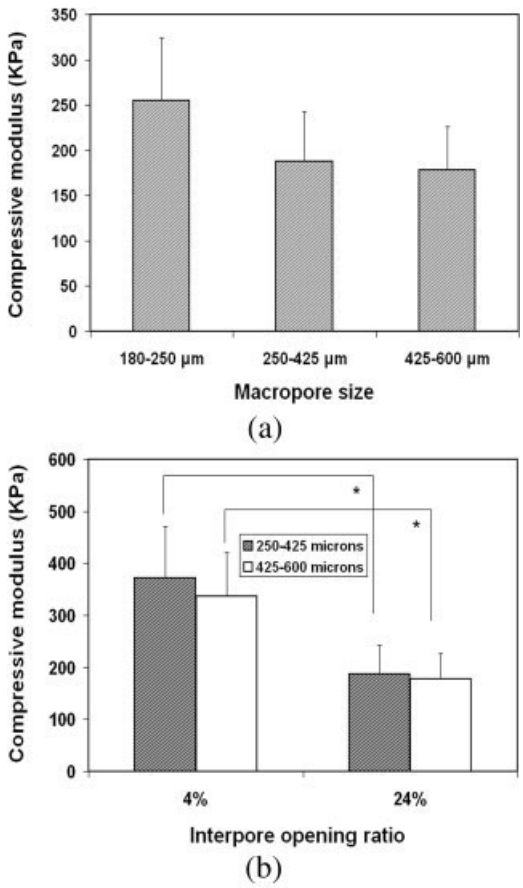

Figure 4. Effect of (a) macropore size and (b) interpore opening ratio on mechanical properties of the scaffold.

$CaCl_2$, and Na_2SO_4 in deionized water and buffered at a pH value of 7.4 at 37°C with tri-(hydroxymethyl) aminomethane [$(CH_2OH)_3CNH_2$] and hydrochloric acid (HCl). The inorganic ion concentrations (Na^+ 213, K^+ 7.5, Mg^{2+} 2.3, Ca^{2+} 3.8, Cl^- 223, HCO_3^- 27, HPO_4^{2-} 1.5, and SO_4^{2-} 0.8 m*M*) were 1.5 times those of human blood plasma. The SBF solution was changed every other day. After incubation at 37°C for a designated time period, scaffolds were removed from SBF, rinsed with distilled water twice overnight, and vacuum dried.

Morphological characterization

The porous morphologies of the scaffolds were examined with scanning electron microscopy (SEM) (Hitachi S-3200N and Philips XL30 FEG) at 15–20 kV. The samples were cut by a razor blade or fractured after liquid nitrogen treatment and coated with gold for 150 s using a sputter coater (Desk-II, Denton Vacuum). Overall porosity was calculated using the method described by Wei and Ma.[15] Interpore opening size and interpore opening ratio (IOR) were determined from SEM images according to Chen and Ma.[19] IOR is defined as the ratio of interpore opening area to macropore surface area in a scaffold. At least 30 pores in a few representative SEM images were analyzed. For energy-dispersive spectroscopy (EDS), scaffold samples without gold coating were used to characterize the composition of apatite particles under an environmental mode.

Surface area measurement

The specific surface area (A_{BET}) measurement was performed on nanofibrous PLLA scaffolds using a BELSORP-mini apparatus (BEL Japan). Adsorption/desorption isotherms of samples were obtained using nitrogen as the adsorbate and liquid nitrogen as cooling medium. Surface area of nanofibrous scaffolds was calculated from Brunauer–Emmett–Teller (BET) plot of adsorption/desorption isotherm using adsorption points in the P/P_0 range of 0.1–0.3 (BELSORP-mini analysis software).

Mechanical test

The compressive mechanical properties of the scaffolds were measured using a MTS Synergie 200 mechanical tester (MTS systems, Eden Prairie, Minnesota). Scaffolds with dimensions of 17.5 ± 0.5 mm in diameter and 3 mm in thickness were used. Five specimens were tested for each sample. The compressive modulus was defined as the initial linear modulus on the stress–strain curves. A two-tail Student's *t*-test (unequal variances) was performed to determine the statistical significance ($p < 0.05$) of the differences in mechanical properties.

RESULTS

Morphological properties

Macroporous and nanofibrous scaffolds have been prepared using sugar template leaching and phase-separation techniques following the steps depicted in Figure 1(a–d). Figure 1(e,f) show the typical morphology of scaffolds prepared using sugar spheres with a diameter of 250–425 μm (PLLA250) and heat treated at 37°C for 15 min. The scaffold has macropores 250–425 μm in diameter, an average interpore opening size of 116 μm, and nanofibers with an average diameter in the order of 100 nm. By varying sugar sphere size and assembly conditions (heat treatment temperature and time), one can easily control the macropore size, the interpore opening size, and interpore opening area ratio (Table 1). Figure 2 shows the morphology of scaffolds with different macropore sizes. Under the same assembly conditions (37°C for 15 min), the resulting scaffolds have the same high porosity of 98% despite the differences in macropore size. With the same IOR of about 20%, the average interpore opening sizes are substantially different, varying from 71 μm

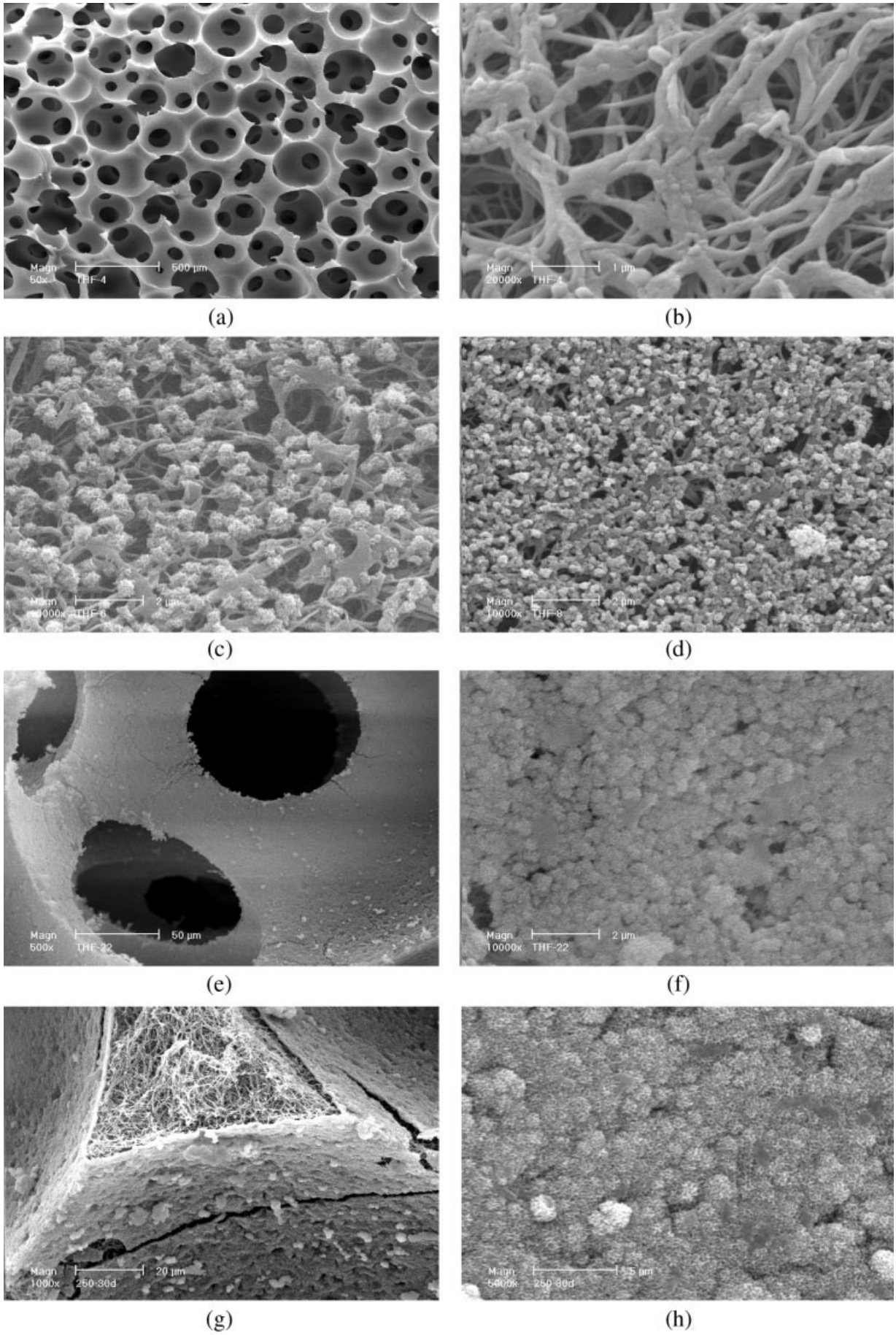

Figure 5. SEM micrographs of nanofibrous PLLA scaffolds incubated in ×1.5 SBF for varying times: (a, b) 4 days (at low and high magnifications); (c) 6 days; (d) 8 days; (e, f) 22 days, and (g, h) 30 days.

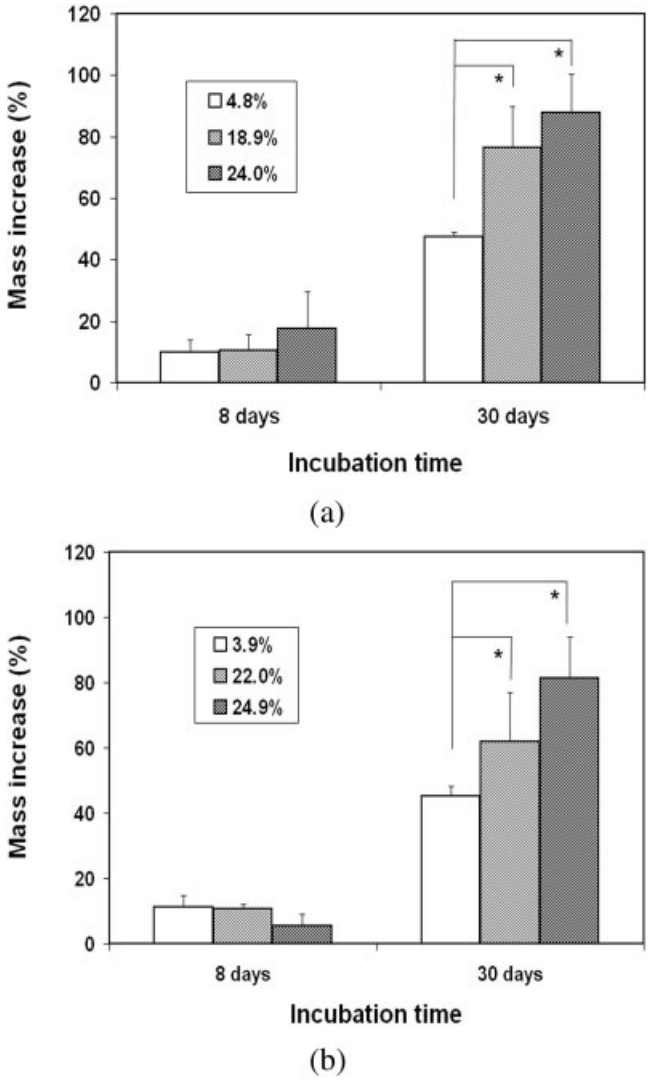

Figure 6. Effect of interpore opening ratio (IOR) on apatite formation on the scaffolds in the SBF. Macropore sizes of the scaffolds: (a) 250–425 μm and (b) 425–600 μm. *$p < 0.05$. Legends in figures indicate the IOR of the scaffold.

for scaffolds prepared with 180–250 μm sugar spheres to 158 μm for scaffolds prepared with 425–600 μm sugar spheres. The IOR is controlled by the sugar sphere assembling conditions, mainly the heat treatment temperature and time (Fig. 3). The IORs of 4.8% and 29.1% are achieved for PLLA scaffolds without heat treatment and with heat treatment at 57°C for 15 min, respectively (Table 1).

Macroporous and nanofibrous PLLA scaffold has a very high surface area of 90–110 m^2/g, regardless of the macropore sizes and IORs. The nanofibrous structure contributes substantially to the large surface area of the scaffold because the nonnano-fibrous equivalent (scaffold with similar macroporous structure but without nanofibrous networks) has a surface area lower than 0.1 m^2/g (data not shown).

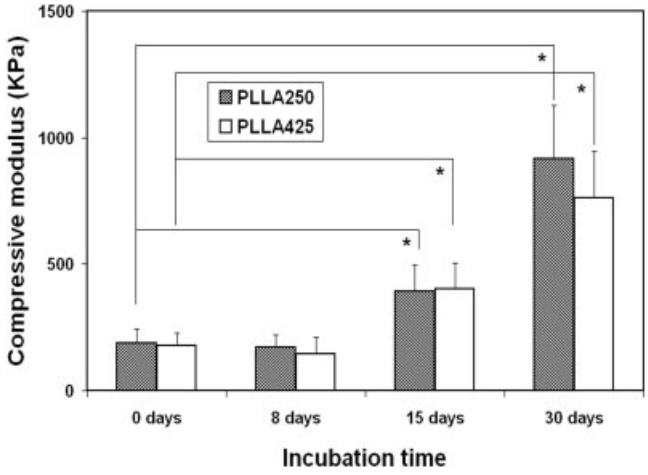

Figure 7. Compressive modulus of the scaffolds after incubation in SBF for varying times. *$p < 0.05$ versus control scaffold (before incubation).

Mechanical properties

For the measurement of mechanical properties, all nanofibrous PLLA scaffolds have a similar porosity of about 98%. The mechanical properties are examined against macropore size [Fig. 4(a)] and IOR of the scaffolds [Fig. 4(b)]. The difference in compressive modulus between scaffolds with different macropore sizes is not statistically significant ($p > 0.05$), although scaffolds with smaller macropore size (180–250 μm) show a slightly higher compressive modulus than scaffolds with larger macropore sizes (250–425 μm or 425–600 μm) [Fig. 4(a)]. A larger IOR results in a lower compressive modulus [Fig. 4(b)].

Growth of bone-like apatite

In vitro growth of bone-like apatite particles on scaffolds is evaluated using SEM, EDS, mechanical prop-

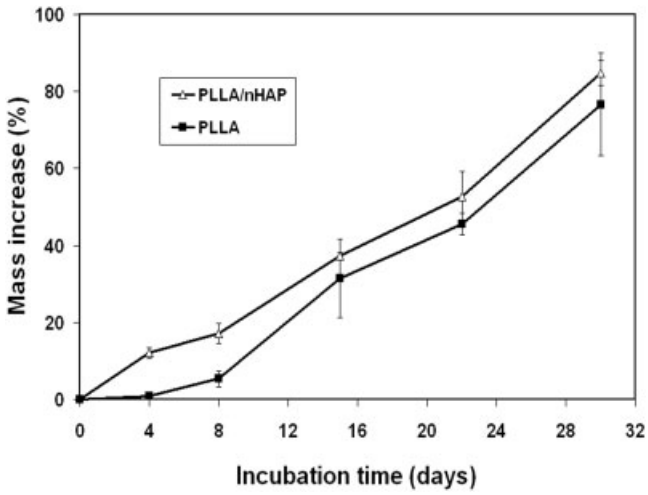

Figure 8. Mass increase of nanofibrous PLLA and PLLA/nHAP scaffolds over incubation time in ×1.5 SBF.

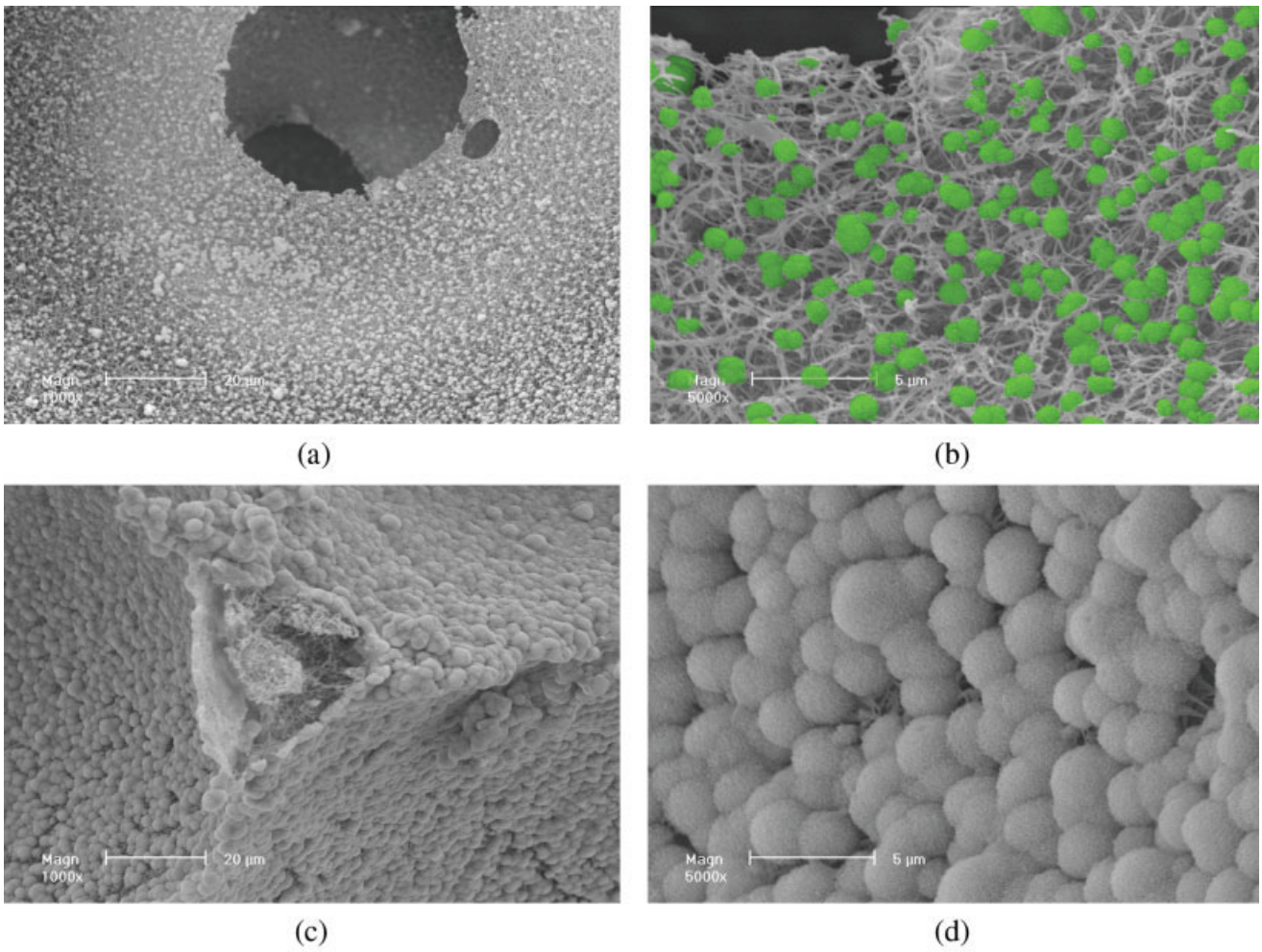

Figure 9. SEM micrographs of nanofibrous PLLA/nHAP (90:10) composite scaffolds incubated in ×1.5 SBF for varying times. (a, b) 4 days [(b) is a portion of (a) at a higher magnification in which the newly formed bone-like apatite is colored green]; (c, d) 30 days. [Color figure can be viewed in the online issue, which is available at www.interscience.wiley.com.]

erties, and mass increase as a function of incubation time. Figure 5 shows SEM micrographs of apatite growth on PLLA nanofibrous scaffolds after varying times of incubation in SBF. Substantial amounts of bone-like apatite crystals are formed on nanofibrous PLLA scaffolds after 6 days of incubation in SBF [Fig. 5(c)]. The deposited apatite particles grow into a few hundred nanometers in size and have nanostructured surface features. The underlying nanofibers become hardly observable after 15 days of incubation. Further incubation in the SBF leads to a continuous apatite layer formation, covering all inner pore wall surfaces [Fig. 5(e–h)]. The interconnected macroporous structure of the scaffolds is maintained, which is important for cell migration and mass transport when used for tissue regeneration. There is not appreciable apatite formation in the bulk of nanofiber network away from macropore wall surfaces [Fig. 5(g)]. The macropore size (from 180–250 μm, 250–425 μm to 425–600 μm) of the scaffold does not have significant effect on the rate and amount of apatite deposition (data not shown). However, the interpore opening size and IOR affect the apatite growth on scaffolds at long incubation times. Scaffolds with larger interpore openings (158 μm) and higher IOR (24%) allow significantly more apatite deposition than those with smaller interpore openings (58 μm) and lower IOR (4%) (Fig. 6). Significantly higher compressive modulus is observed for composite scaffold when apatite particles become a continuous layer covering the entire pore wall surfaces after 15 days or longer incubation times in SBF (Fig. 7).

Preincorporation of nHAP particles in polymer scaffolds (even at a low content of 10 w/w%) induces greater amounts of apatite formation in SBF as compared to pure polymer scaffolds (Fig. 8). Substantial amounts of apatite crystals are grown on PLLA/nHAP composite scaffolds after 4 days of incubation in SBF [Fig. 9(a,b)]. At this time, there is a negligible amount of apatite formation on pure polymer scaffolds [Fig. 5(a,b)]. This is also confirmed by EDS spectra (Fig. 10). There are significant increases of Ca and

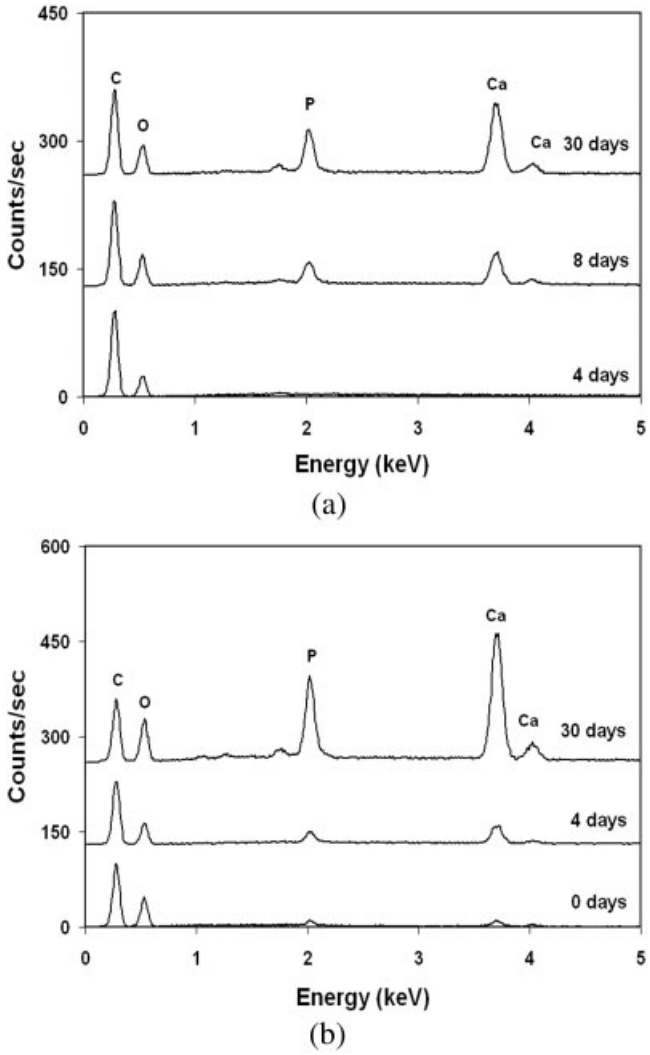

Figure 10. EDS spectra of apatite deposited on (a) PLLA and (b) PLLA/nHAP scaffolds. The peak of carbon element in each curve was normalized to 100 counts/s.

P elements in the PLLA/nHAP (10 w/w% nHAP) scaffolds after 4 days of incubation in the SBF. However, the Ca and P elements are not detectable for pure PLLA scaffolds after 4 days of incubation in the SBF. The size and morphology of apatite particles on PLLA/nHAP nanocomposite scaffolds (Fig. 9) are different from those on pure PLLA scaffolds (Fig. 5). The apatite particle size increases from 0.8–1 μm at day 4 to 2–2.5 μm at day 30 for PLLA/nHAP scaffolds while the apatite particles on PLLA scaffolds are less than 1 μm in diameter after 30 days of incubation.

DISCUSSION

To achieve the ultimate goal of tissue engineering, generating clinically useful tissue and organ replacement, great efforts have been made in scaffold designs to regulate cell behavior including attachment, migration, proliferation, and differentiation on a scaffold.[9,13] A tissue engineering scaffold should have high porosity, suitable macropore size, well-controlled interpore openings, appropriate surface morphologies, and suitable mechanical properties as well as bioactivity. Several techniques have been developed to fabricate 3D porous scaffolds.[3,5,20] However, there is still a limited capacity of controlling scaffold structural features and functions. We have presented in this work, a phase separation and sugar sphere leaching technique to prepare highly porous 3D scaffold with good mechanical properties, controlled pore geometries, and a nanofibrous pore wall surface morphology. In this scaffold system, macropores and interpore openings are designed to facilitate initial cell seeding and mass transfer during *in vitro* cell culture, and nanofibrous pore wall structures for better cell attachment, proliferation, and differentiation functions. The insufficient interconnected macroporosity of certain scaffolds has been shown to limit cell colonization to the very superficial layer (~240 μm from surface of a 1.9 mm-thick scaffold).[6] The presence of interpore openings, therefore, is considered to be essential for cellular activities,[2] including uniform cell seeding throughout the scaffold *in vitro* and angiogenesis *in vivo*. The newly developed technique can be employed to fabricate a variety of polymers into 3D scaffolds with a high porosity and well-controlled macropores and interpore openings.

An attractive feature of the technique is that nanofibrous structure has been incorporated into macropore walls of the 3D PLLA scaffolds [Fig. 1(f)]. The density of the nanofibers can be modulated by phase-separation parameters such as polymer solution concentration and phase-separation temperature. The nanofibrous structure, which mimics the main natural bone extracellular matrix (ECM) component (collagen) in size, has been demonstrated to improve cell attachment[9] and proliferation.[21] The combination of interconnected macroporous and nanofibrous features in a 3D scaffold would provide a better environment for cell growth and differentiation.

To be effectively used for bone tissue regeneration, it is beneficial that a scaffold promotes bone-like apatite formation when in contact with physiological fluid. To evaluate the bioactivity of the novel macroporous and nanofibrous PLLA scaffolds developed in this study, we have investigated their ability to form bone-like apatite in a SBF. Apatite particles were deposited uniformly throughout the macroporous and nanofibrous PLLA scaffolds. With increasing incubation time, the density of the apatite layer increased. Noting very uniform growth of apatite layers throughout the macroporous and nanofibrous PLLA scaffolds but not on the scaffolds without the nanofeatures,[16,22] it is likely that the physical and surface characteristics

of the scaffold (macropores, interpore openings, and nanotopography) affect the formation kinetics and morphology of apatite layers.[22] The preincorporation of nHAP greatly altered the apatite growth profile; it eliminated an induction time for stable nuclei formation and accelerated apatite growth. It also led to greater mass increase and larger apatite particle size, which may be attributed to the increased ionic availability, possibly due to the lower number of nuclei (preincorporated nHAP) in PLLA/nHAP scaffolds.

Plasma spraying process, a most commonly used conventional HAP-coating technique,[23] is not appropriate for biodegradable 3D scaffold because of heat generation during the process and its inability to cover the entire surfaces of the deep internal pores because of the nature of the process. Furthermore, possible overcoating on the surface of the porous structure with HAP generally alters the morphology of the pores by blocking the macropores and interpore openings. In this study, we have developed two different methods to fabricate nanofibrous PLLA/nHAP (direct mixing) or PLLA/apatite (biomimetic coating from SBF) nanocomposite scaffolds. The biomimetic method created a macroporous PLLA/apatite nanocomposite scaffold with preserved open macroporous structure and improved mechanical properties. In addition, the biomimetic PLLA/apatite nanocomposite scaffold provides an environment that mimics the natural bone matrix more closely (with polymer nanofibers and apatite nanocrystals) and may enhance bone tissue regeneration.

CONCLUSIONS

Macroporous and nanofibrous PLLA scaffolds are prepared by a novel phase separation and sugar sphere template leaching technique. The combined technique has shown great control over macropore size, interpore opening size, as well as pore wall morphologies of 3D scaffolds. Bone-like apatite layer has grown uniformly throughout 3D nanofibrous scaffold after SBF incubation, which has not only demonstrated the bioactivity of the macroporous and nanofibrous scaffold but has also provided a method to generate biomimetic surfaces. The resulting scaffolds should have better osteoconductivity and improved mechanical properties for bone tissue engineering applications.

References

1. Ma PX. Scaffolds for tissue fabrication. Mater Today 2004;7(5):30–40.
2. Ma PX. Tissue engineering. In: Kroschwitz J, editor. Encyclopedia of Polymer Science and Technology. New York: Wiley; 2005;12:261–291.
3. Zhang RY, Ma PX. Poly(α-hydroxyl acids) hydroxyapatite porous composites for bone-tissue engineering. I. Preparation and morphology. J Biomed Mater Res 1999;44:446–455.
4. Ma PX, Zhang RY. Synthetic nano-scale fibrous extracellular matrix. J Biomed Mater Res 1999;46:60–72.
5. Ma PX, Zhang RY. Microtubular architecture of biodegradable polymer scaffolds. J Biomed Mater Res 2001;56:469–477.
6. Ishaug SL, Crane GM, Miller MJ, Yasko AW, Yaszemski MJ, Mikos AG. Bone formation by three-dimensional stromal osteoblast culture in biodegradable polymer scaffolds. J Biomed Mater Res 1997;36:17–28.
7. Liu XH, Ma PX. Polymeric scaffolds for bone tissue engineering. Ann Biomed Eng 2004;32:477–486.
8. Lu JX, Flautre B, Anselme K, Hardouin P, Gallur A, Descamps M, Thierry B. Role of interconnections in porous bioceramics on bone recolonization in vitro and in vivo. J Mater Sci Mater Med 1999;10:111–120.
9. Woo KM, Chen VJ, Ma PX. Nano-fibrous scaffolding architecture selectively enhances protein adsorption contributing to cell attachment. J Biomed Mater Res A 2003;67:531–537.
10. Webster TJ, Waid MC, McKenzie JL, Price RL, Ejiofor JU. Nano-biotechnology: Carbon nanofibres as improved neural and orthopaedic implants. Nanotechnology 2004;15:48–54.
11. Geesink RGT, Degroot K, Klein C. Bonding of bone to apatite-coated implants. J Bone Joint Surg Br 1988;70:17–22.
12. Cook SD, Thomas KA, Dalton JE, Volkman TK, Whitecloud TS, Kay JF. Hydroxylapatite coating of porous implants improves bone ingrowth and interface attachment strength. J Biomed Mater Res 1992;26:989–1001.
13. Ma PX, Zhang RY, Xiao GZ, Franceschi R. Engineering new bone tissue in vitro on highly porous poly(α-hydroxyl acids)/hydroxyapatite composite scaffolds. J Biomed Mater Res 2001;54:284–293.
14. Woo KM, Zhang RY, Deng HY, Ma PX. Protein-mediated osteoblast survival and migration on biodegradable polymer/hydroxyapatite scaffolds. Trans Soc Biomater 2002;25:605.
15. Wei G, Ma PX. Structure and properties of nano-hydroxyapatite/polymer composite scaffolds for bone tissue engineering. Biomaterials 2004;25:4749–4757.
16. Zhang RY, Ma PX. Porous poly(L-lactic acid)/apatite composites created by biomimetic process. J Biomed Mater Res 1999;45:285–293.
17. Thomson RC, Yaszemski MJ, Powers JM, Mikos AG. Hydroxyapatite fiber reinforced poly(α-hydroxy ester) foams for bone regeneration. Biomaterials 1998;19:1935–1943.
18. Zhang RY, Ma PX. Synthetic nano-fibrillar extracellular matrices with predesigned macroporous architectures. J Biomed Mater Res 2000;52:430–438.
19. Chen VJ, Ma PX. Nano-fibrous poly(L-lactic acid) scaffolds with interconnected spherical macropores. Biomaterials 2004;25:2065–2073.
20. Mikos AG, Thorsen AJ, Czerwonka LA, Bao Y, Langer R, Winslow DN, Vacanti JP. Preparation and characterization of poly(L-lactic acid) foams. Polymer 1994;35:1068–1077.
21. Xu CY, Inai R, Kotaki M, Ramakrishna S. Aligned biodegradable nanotibrous structure: A potential scaffold for blood vessel engineering. Biomaterials 2004;25:877–886.
22. Zhang RY, Ma PX. Biomimetic polymer/apatite composite scaffolds for mineralized tissue engineering. Macromol Biosci 2004;4:100–111.
23. Sun LM, Berndt CC, Gross KA, Kucuk A. Material fundamentals and clinical performance of plasma-sprayed hydroxyapatite coatings: A review. J Biomed Mater Res 2001;58:570–592.